JOURNAL OF SOLID STATE CHEMISTRY 120, 146–150 (1995)

Oxygen Nonstoichiometry of $(Nd_{2/3}Ce_{1/3})_4(Ba_{2/3}Nd_{1/3})_4Cu_6O_{16+x}$

M. V. Patrakeev, I. A. Leonidov, A. A. Lakhtin, and V. L. Kozhevnikov[1]

Institute of Solid State Chemistry, Ural Division of Russian Academy of Science, Pervomaiskaia 91, Ekaterinburg 620219, Russian Federation

and

A. V. Nikolaev

Russian–French Joint Venture "Quorus," Lunacharskogo 81, Ekaterinburg 620075, Russian Federation

Received February 13, 1995; in revised form June 27, 1995; accepted June 28, 1995

The equilibrium oxygen content of $(Nd_{2/3}Ce_{1/3})_4(Ba_{2/3}Nd_{1/3})_4Cu_6O_{16+x}$ was measured by coulomeric titration in the temperature range 550–820°C and at oxygen pressures between 10^{-3} and 1 atm. From the results, the partial molar enthalpy and entropy of oxygen were calculated as functions of the oxygen content. The data were explained based on a point defects model and the equilibrium constants of the redox and charge disproportionation reactions involved were derived. A phase transition near the point $x \approx 1.83$, which nominally corresponds to one trivalent copper cation per elementary unit, was observed. © 1995 Academic Press, Inc.

INTRODUCTION

The family of solid solutions $(Ln_{1-y}Ce_y)_4(Ba_{1-z})_4Cu_6O_{16+x}$, where Ln is a rare earth or Y, with the superconducting transition temperature of about 40 K was identified by Sawa *et al.* (1). The tetragonal elementary unit of $(Ln_{1-y}Ce_y)_4(Ba_{1-z})_4Cu_6O_{16+x}$ consists of metal–oxygen layers stacked in the c direction. The two layers have the composition $CuO_{x/2}$ and are functionally equivalent to the basal plane layer CuO_x in the $YBa_2Cu_3O_{6+x}$ compound (1–4). As was shown in further studies, the value of the oxygen index, x, depends on the cation composition (5) and, to a substantial degree, on oxygen pressure during anneals (3, 5). The thermogravimetric data (3) indicate a wide range of reversible change of x depending on temperature, T, and oxygen partial pressure, p_{O_2}. A more detailed study of the change in oxygen content as a function of temperature and oxygen fugacity is of both practical and theoretical interest. Not only does it enable a reproducible synthesis of the material with the desired oxygen content, but it also serves as a basis for the interpretation of other high-temperature experiments (measurements of conductivity, thermopower, etc.). Moreover, the thermodynamic analysis of the $x(T, p_{O_2})$ behavior is of interest because it provides valuable information on the oxygen–oxygen interactions in the compound and it helps one to draw some conclusions on the electronic structure of the oxide (6).

In this paper, we report data on the equilibrium oxygen content in $(Nd_{2/3}Ce_{1/3})_4(Ba_{2/3}Nd_{1/3})_4Cu_6O_{16+x}$ obtained by means of coulometric titration using a solid electrolyte of yttria-stabilized zirconia over a wide range of oxygen pressures and temperatures. From the experimental results, the partial thermodynamic functions of oxygen in $(Nd_{2/3}Ce_{1/3})_4(Ba_{2/3}Nd_{1/3})_4Cu_6O_{16+x}$ were derived. The parameters influencing the high-temperature equilibrium between $(Nd_{2/3}Ce_{1/3})_4(Ba_{2/3}Nd_{1/3})_4Cu_6O_{16+x}$ and gas phase oxygen were estimated by applying physical and chemical principles.

EXPERIMENTAL

The specimen of $(Nd_{2/3}Ce_{1/3})_4(Ba_{2/3}Nd_{1/3})_4Cu_6O_{16+x}$ was synthesized via solid-state reaction using reagent grade powders of Nd_2O_3 (99.996%), CeO_2 (99.95%), $BaCO_3$ (99.93%), and CuO (99.99%). X-ray powder diffraction was used for phase purity control before and after high-temperature experiments. In both cases, the specimen was found to be a single tetragonal phase. The room temperature lattice parameters were $a = 3.859(5)$ and $c = 28.48(2)$ Å. Mass percentages of Nd, Ba, Ce, and Cu in the prepared specimen were determined by chemical analysis and were consistent with the nominal composition. The oxygen content in the prepared specimen was determined using a Setaram TG-92 thermoanalyzer in the 5% H_2 + 95% Ar gas mixture flow; see Fig. 1. The copper was reduced to metal under the experimental conditions while the Nd, Ce, and Ba cations preserved their oxidation states. Therefore, the final oxygen content in the reduced sample was as-

[1] To whom correspondence should be addressed.

0022-4596/95 $12.00

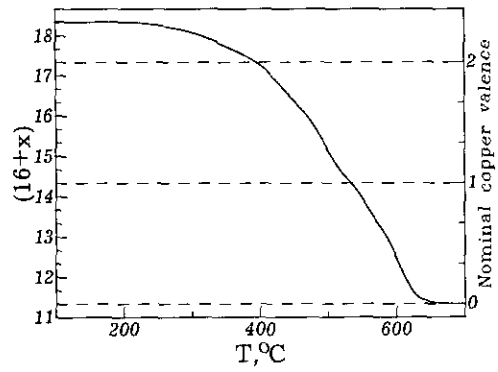

FIG. 1. The mass change of the $(Nd_{2/3}Ce_{1/3})_4(Ba_{2/3}Nd_{1/3})_4Cu_6O_{16+x}$ specimen in the 5% H_2 + 95% Ar gas mixture at 5°/min heating.

sumed to be equal to $11\frac{1}{3}$ at the end of the TG-run. Hence, the initial oxygen content, $16 + x$, in the specimen was determined to be equal to 18.34. Another isobar measured with the same TG-apparatus at $p_{O_2} = 0.21$ atm was used to determine the x value of the reference point for the coulometric experiments.

The setup for coulometric titration was computer controlled. The electrical parameters of the experiment were measured by a highly precise Solartron 7081 voltmeter. The electrochemical interface Solartron 1286 supplied direct current. The experimental cell (inner diameter 8 mm, outer diameter 10 mm, height 20 mm) was made of cubically stabilized zirconia. Two pairs of platinum electrodes were attached to the outside and inside of the cell and served as the electrochemical oxygen sensor (electrode area was about 3 mm^2) and the pump (electrode area was about 1 cm^2). The pump current was in the range 0.2–2.0 mA. The duration of the current was 2–20 min. The equilibration time was 15–150 min, depending on experimental conditions. About 500 mg of the specimen was placed in a thin-walled corundum liner to prevent direct contact between the powder and the zirconia. Then the liner was placed in the cell. The average size of grains in the powder was about 10 μm. The cell was sealed with a zirconia lid and high-temperature glass in a flow of oxygen at 900°C. The cell temperature was controlled by a PtRh(30%)–PtRh(6%) thermocouple. The reference electrode of the oxygen sensor was 1 atm of air during all experiments.

The next stage of the experiment included obtaining a representative set of data in isothermal runs. A reference data set consisted of 15 points, each corresponding to a different temperature. The equilibrium oxygen pressure for each point was measured with the oxygen sensor. The corresponding value of x for the point under measurement was calculated from the (T, p_{O_2}, x) parameters of the previous point applying the ideal gas law for the cell's free volume. The criterion for the achievement of equilibrium for each point was a steady value of the e.m.f. of the oxygen sensor within ± 5 μV for 1 hr.

Representative sets of data were obtained in isothermal runs. A small amount of oxygen was added or removed from the cell by passing an appropriate direct current through the electrodes of the oxygen pump for a definite time. After equilibration, the corresponding value of x was calculated from T, p_{O_2}, and the parameters of the preceding point using the Faraday law and the ideal gas law. Then the next quantity of electric charge was allowed to pass through the electrodes of the pump. Upon achievement of the desirable limit of p_{O_2}, the temperature and the current direction were changed and the cycle of the measurements was continued. Each isotherm obtained in these runs was corrected by comparison with the previously measured reference point to avoid an accumulation of the experimental error which inevitably enters such measurements owing to the small electronic conductance of the zirconia electrolyte.

ENTHALPY AND ENTROPY

In Fig. 2 the p–x isotherms for the oxygen solution in $(Nd_{2/3}Ce_{1/3})_4(Ba_{2/3}Nd_{1/3})_4Cu_6O_{16+x}$ are shown in the temperature range 550–820°C and at oxygen pressures between 10^{-3} and 1 atm. The uncertainty in the oxygen content, x, at the initial reference point (T = 784°C, p_{O_2} = 0.21 atm, x = 1.733) is estimated to be on the order of 0.03. It arises owing to errors in the TG microbalance weighing. The uncertainties in the oxygen content determination relative to the reference point are estimated to be about 0.005. These uncertainties enter the data because of errors in temperature readings and in measurements of the cell's free volume, changes of atmospheric pressure,

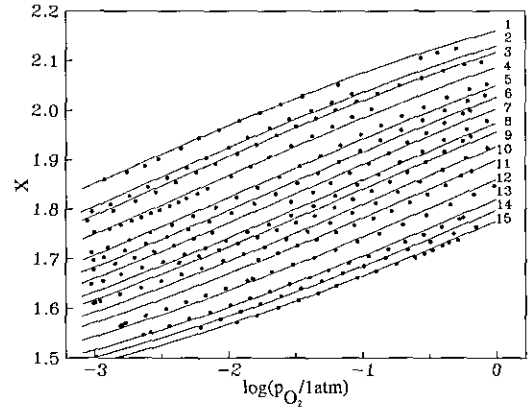

FIG. 2. The p_{O_2}–T–x diagram for $(Nd_{2/3}Ce_{1/3})_4(Ba_{2/3}Nd_{1/3})_4Cu_6O_{16+x}$. The circles show experimental points. The straight lines represent calculations according Eq. [13]. The isotherms correspond to the temperatures (°C): 1, 550; 2, 572; 3, 581; 4, 601; 5, 625; 6, 640; 7, 655; 8, 674; 9, 686; 10, 706; 11, 725; 12, 753; 13, 784; 14, 802; 15, 820.

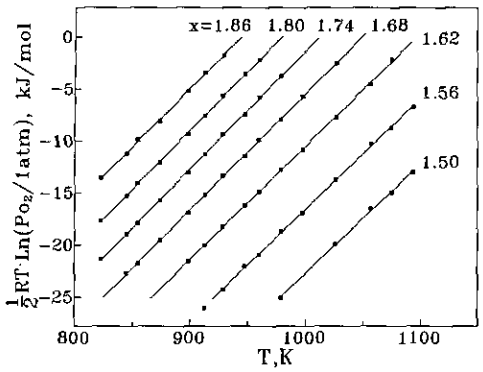

FIG. 3. The plots of the partial free energy of oxygen in $(Nd_{2/3}Ce_{1/3})_4(Ba_{2/3}Nd_{1/3})_4Cu_6O_{16+x}$ vs temperature at several fixed values of x. The straight lines show the results of the least-square fittings according to Eq. [1].

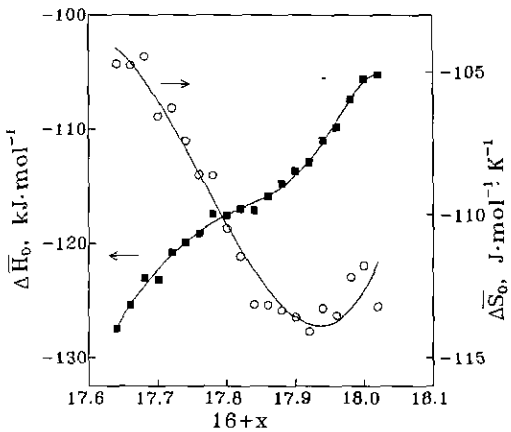

FIG. 4. The plots of $\Delta\bar{H}_0$ and $\Delta\bar{S}_0$ vs oxygen content in $(Nd_{2/3}Ce_{1/3})_4(Ba_{2/3}Nd_{1/3})_4Cu_6O_{16+x}$.

and small oxygen leaks through cell's walls (owing to the small electron conductance of the zirconia). The data corresponding to the experimental isotherms were smoothed by interpolation and used to calculate the partial molar enthalpy, $\Delta\bar{H}_0$, and entropy, $\Delta\bar{S}_0$, of oxygen in $(Nd_{2/3}Ce_{1/3})_4(Ba_{2/3}Nd_{1/3})_4Cu_6O_{16+x}$ assuming that these quantities are independent of temperature in the investigated temperature range:

$$\Delta\bar{G}_0(x, T) = \Delta\bar{H}_0(x) - T\Delta\bar{S}_0(x) = \tfrac{1}{2}RT \ln p_{O_2}. \qquad [1]$$

The functions $\Delta\bar{H}_0(x)$ and $\Delta\bar{S}_0(x)$ were determined by linear least-squares fittings from the temperature dependencies of the partial free energy, $\Delta\bar{G}_0$, at fixed x. In Fig. 3 several calculated isoconcentrates of $\Delta\bar{G}_0$ vs temperature are plotted together with straight lines showing the best fit to the corresponding isoconcentrates. The partial molar entropy is determined by the slope of these lines, while partial molar enthalpy is given by the intercept of these lines with the $\Delta\bar{G}_0$ axis at $T = 0$. To limit the inaccuracy toward the end points of the oxygen content range, the calculations were restricted to the oxygen concentrations for which more than four data points of $\Delta\bar{G}_0$ (x = const, T) were available. The obtained $\Delta\bar{H}_0(x)$ and $\Delta\bar{S}_0(x)$ functions are presented in Fig. 4. It should be clear that the points of these functions at fixed x's correspond to the average values over the investigated temperature range.

EQUILIBRIUM DEFECTS MODEL

The partial molar entropy of oxygen in $(Nd_{2/3}Ce_{1/3})_4(Ba_{2/3}Nd_{1/3})_4Cu_6O_{16+x}$ decreases sharply (to a greater extent than the value of the gas constant R) as x increases from 1.64 to 1.83 while the enthalpy increases. One possible reason for such behavior may be a transition from the filling of one oxygen sublattice available for the oxygen exchange to the filling of another energetically less favorable oxygen sublattice, similar to the case of the O(1) and O(5) basal plane oxygen sites in the $YBa_2Cu_3O_{6+x}$ orthorhombic phase. However, neutron powder diffraction data (2, 3) show that all four oxygen positions which participate in the oxygen exchange in the $(Nd_{2/3}Ce_{1/3})_4(Ba_{2/3}Nd_{1/3})_4Cu_6O_{16+x}$ elementary unit are structurally (and therefore energetically) equivalent. Moreover, our experimental data show that the sharp change of the thermodynamic functions occurs in the vicinity of the point $x_c = 1.83$ but not near the point $x = 2.00$ which would correspond to a half filling of the oxygen positions. This behavior is clearly seen in Fig. 5, where the experimental data from Fig. 2 are replotted as isobars. The cusps of the isobars in the figure are located near the line of the oxygen composition $x = x_c$. This critical oxygen content corresponds nominally to one Cu^{3+} cation per elementary unit. Hence, it is likely that the transition is connected with some change in the electronic structure. For example, in the rigid-band approx-

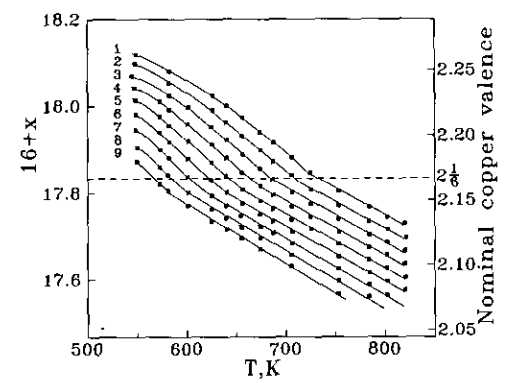

FIG. 5. The plots of the oxygen contents vs temperature at fixed oxygen pressures (in $-\log(p_{O_2}/\text{atm})$ units): 1, 0.39; 2, 0.69; 3, 0.99; 4, 1.29; 5, 1.59; 6, 1.89; 7, 2.19; 8, 2.49; 9, 2.79.

imation to the band structure description, such changes in the $p-T-x$ diagram near the x_c point might be attributed to the shift of the Fermi level from one area of rather high density of states to another area divided from the first by a gap. In accordance with these arguments, we write the chemical composition of the compound as

$$Nd_4^{3+}Ba_{8/3}^{2+}Ce_{4/3}^{4+}Cu_4^{2+}O_{16}^{2-}(Cu_{1+e-h}^{2+}Cu_{1-e+h}^{3+}Vo_{4-x}O_x^{2-}), \quad [2]$$

where e and h denote concentrations of electrons and electron holes, respectively, Vo is the concentration of oxygen vacancies, and the parentheses enclose the part of the elementary unit which depends on oxygen pressure and temperature. For simplicity, the present formalism is based on Cu^{3+} ions. However, it should be emphasized that independent of whatever charge transfer model is adopted, it does not have an effect on the final results assuming that the total number of the states available for the electrons and holes does not depend greatly on the charge transfer model. Based on [2], the lattice electroneutrality requires that

$$e - h = 3\tfrac{2}{3} - 2x. \quad [3]$$

Then, applying Kröger–Vink notation the predominating reaction for the range of the electrons predomination ($x < 1\frac{5}{6}$) is

$$2Cu_{Cu} + O_O = \tfrac{1}{2}O_2(g) + V_O^{\cdot\cdot} + 2Cu'_{Cu}. \quad [4]$$

For the range of the holes predomination at $x > 1\frac{5}{6}$, the corresponding reaction is

$$2Cu^{\cdot}_{Cu} + O_O = \tfrac{1}{2}O_2(g) + V_O^{\cdot\cdot} + 2Cu_{Cu}. \quad [5]$$

Application of the mass action law to reactions [4] and [5] gives

$$K_1 = \frac{[V_O^{\cdot\cdot}][Cu'_{Cu}]^2}{[O_O][Cu_{Cu}]^2} \cdot p_{O_2}^{1/2} \quad [6]$$

$$K_2 = \frac{[V_O^{\cdot\cdot}][Cu_{Cu}]^2}{[O_O][Cu^{\cdot}_{Cu}]^2} \cdot p_{O_2}^{1/2} \quad [7]$$

Taking into account [2], [3], [6], [7], and following the analysis of (7), we obtain

$$(K_1)^{1/2} = u \cdot \frac{h - 2x + 3\frac{2}{3}}{2x - h - 2\frac{2}{3}},$$
$$(K_2)^{1/2} = u \cdot \frac{1-h}{h} \quad \text{with } u = \left\{\frac{4-x}{x} \cdot p_{O_2}^{1/2}\right\}^{1/2}. \quad [8]$$

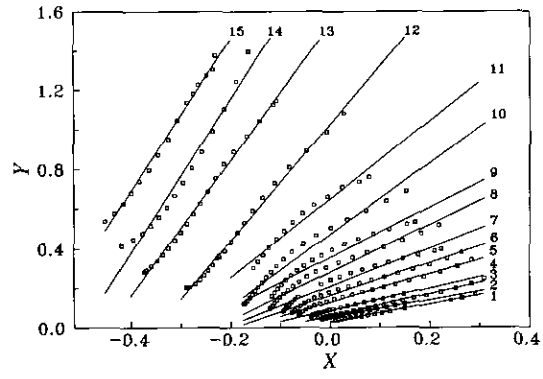

FIG. 6. The $Y-X$ isotherms. The squares correspond to the experimental values plotted according to Eq. [10]. The straight lines show the results of the least-square fittings. The isotherms correspond to the temperatures (°C): 1, 550; 2, 572; 3, 581; 4, 601; 5, 625; 6, 640; 7, 655; 8, 674; 9, 686; 10, 706; 11, 725; 12, 753; 13, 784; 14, 802; 15, 820.

The exclusion of the concentration of holes from Eq. [8] results in the isotherm equation

$$Y = A + B \cdot X, \quad [9]$$

where

$$Y = u^2 \cdot \frac{4\frac{2}{3} - 2x}{2x - 2\frac{2}{3}}, X = u \cdot \frac{2x - 3\frac{2}{3}}{x - 2\frac{2}{3}},$$
$$A = (K_1K_2)^{1/2}, B = (K_1)^{1/2} + (K_2)^{1/2}. \quad [10]$$

The $Y-X$ representation of the experimental isotherms together with the straight lines obtained by the least-squares fittings is given in Fig. 6. The values of A and B are positive for all the lines, in full agreement with Eq. [10]. Some deviations from linearity do appear for the isotherms near the x_c point (where $X = 0$). However, they are not too great. Therefore, this simple model of disordering can be accepted as valid, at least as a first approximation, for the entire range of the external parameters investigated.

The equilibrium constants K_1 and K_2 can be determined from the coefficients A and B. The expressions for A and B are symmetrical to the permutation of K_1 and K_2, as can be seen from Eqs. [10]. Therefore, two variants of plotting over experimental points are possible; see Fig. 7. This situation differs from the case of the corresponding equation for $YBa_2Cu_3O_{6+x}$ obtained previously (7). Let us consider the difference between these two possibilities in more detail. The equilibrium constant, K_3, of the charge disproportionation reaction (excitation of the electron and electron hole),

$$2Cu_{Cu} = Cu^{\cdot}_{Cu} + Cu'_{Cu}, \quad [11]$$

can be expressed as

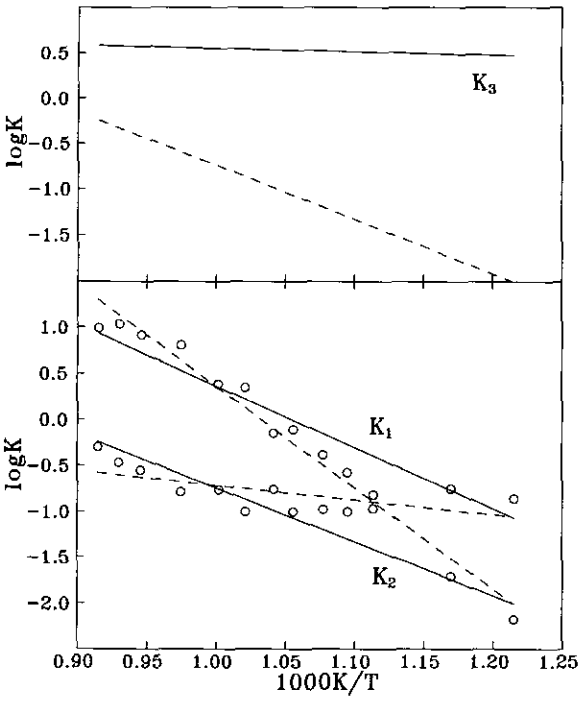

FIG. 7. Arrhenius plots of the equilibrium constants K_1, K_2, and K_3. The solid lines correspond to the forbidden gap of 900 K (see Eq. [13]). The dashed lines correspond to the forbidden gap of 11,000 K.

$$K_3 = [Cu_{Cu}^{\cdot}][Cu_{Cu}^{\prime}][Cu_{Cu}]^{-2} = (K_1/K_2)^{1/2}. \qquad [12]$$

It follows from Eq. [12] that the enthalpy (the width of the forbidden gap) of the reaction [11] can be obtained as the half-difference of the enthalpies of the reactions [4] and [5]. The width of the forbidden gap for the variant presented by the solid lines in Fig. 7 is 900 K, while it is 11,000 K for the variant presented by the dashed lines. There are no conclusive data in the literature on electrophysical properties of the $(Nd_{2/3}Ce_{1/3})_4(Ba_{2/3}Nd_{1/3})_4Cu_6O_{16+x}$ compound at elevated temperatures which would allow one to define the correct variant. However, the electrical conductivity of this compound and of related compounds below room temperature (1, 4, 5, 8) shows either metallic-like behavior ($\partial\sigma/\partial T < 0$) in the whole temperature range below 300 K or a change from metallic-like behavior to semiconducting behavior ($\partial\sigma/\partial T > 0$). Therefore, the variant with the small forbidden gap of 900 K is more preferable. Moreover, the average middle squared deviation of the calculated values of $\log p_{O_2}$ from the experimental ones over the investigated range of $x(T, p_{O_2})$ is smaller for the variant with the small gap than for the variant with the large gap (0.073 and 0.082, respectively). Hence, the equilibrium constants can be described by the formulas.

$$K_1 = 6.5 \cdot 10^6 \cdot \exp(-14{,}900\, K/T)\ (\mathrm{atm}^{1/2}),$$

$$K_2 = 8.9 \cdot 10^4 \cdot \exp(-13{,}100\, K/T)\ (\mathrm{atm}^{1/2}), \qquad [13]$$

$$K_3 = 8.5 \cdot \exp(-900\, K/T).$$

The isotherms, $x(p_{O_2})$, calculated by using these constants are shown by straight lines in Fig. 2. One can see good agreement between the calculated lines and experimental points which proves validity of the suggested model of disorder in $(Nd_{2/3}Ce_{1/3})_4(Ba_{2/3}Nd_{1/3})_4Cu_6O_{16+x}$. Some deviation between the theory and experiment near x_c may be connected with the accepted approximation of the rigid bands.

CONCLUSION

We have measured the oxygen content in $(Nd_{2/3}Ce_{1/3})_4(Ba_{2/3}Nd_{1/3})_4Cu_6O_{16+x}$ at oxygen pressures between 10^{-3} and 1 atm and temperatures between 550 and 820°C. From the results, the partial molar enthalpy and entropy of oxygen in the solid solution were derived as functions of x. We have shown also that the experimental data can be explained assuming an equilibrium of point defects. The equilibrium constants are quite consistent with the experimental data. The change of the nonstoichiometry, $x(T, p_{O_2})$, behavior near the composition $x = 1\frac{5}{8}$ was explained to be connected with a shift of the Fermi level from one area of rather high density of states to the another area divided with the first with a gap. According to this model, there has to be a change of the dominating electron defects near this composition (electrons vs electron holes). Measurement of the electronic conductivity and thermopower to obtain more insight into the nature of this transition are in progress and will be presented in a future paper.

ACKNOWLEDGMENTS

The authors thank Professor Kenneth R. Poeppelmeier for helpful comments. This research was supported by the Council on the HTSC Problem in Russia under Grant 93133 and by the International Science Foundation under Grant RGG 000.

REFERENCES

1. H. Sawa, K. Obara, J. Akimitsu, Y. Matsui, and Sh. Horiuchi, *J. Phys. Soc. Jpn.* **58,** 2252 (1989).
2. F. Izumi, H. Kito, H. Sawa, J. Akimitsu, and H. Asano, *Physica C* **160,** 235 (1989).
3. D. Kovatcheva, P. Strobel, B. Souletie, and A. W. Hewat, *Physica C* **174,** 280 (1991).
4. T. Wada, A. Ichinose, Y. Yaegashi, H. Yamauchi, and Sh. Takana, *Jpn. J. Appl. Phys.* **28,** L1779 (1989).
5. A. Ichinose, T. Wada, Y. Yaegashi, H. Yamauchi, and Sh. Takana, *Jpn. J. Appl. Phys.* **28,** L1765 (1989).
6. V. I. Tsidilkovskii, I. A. Leonidov, A. A. Lakhtin, and V. A. Mezrin, *Phys. Status Solidi B* **168,** 233 (1991).
7. J. Nowotny and M. Rekas, *J. Am. Ceram. Soc.* **73,** 1048 (1990).
8. T. Wada, A. Ichinose, Y. Yaegashi, H. Yamauchi, and Sh. Takana, *Jpn. J. Appl. Phys.* **29,** L266 (1990).